Effect of thermal radiation on chemically reacting magnetohydrodynamic dusty viscous fluid flow in a porous channel

IOP Conf. Series: Materials Science and Engineering **263** (2017) 062028 doi:10.1088/1757-899X/263/6/062028

Effect of thermal radiation on chemically reacting magnetohydrodynamic dusty viscous fluid flow in a porous channel

B Rushi Kumar, H Thameem Basha, R Sivaraj and N Sandeep
Department of Mathematics, School of Advanced Sciences, VIT University, Vellore – 632014, India

Email: sivaraj.kpm@gmail.com

Abstract. In this paper, we have studied the combined effects of free convective heat and mass transfer on an unsteady MHD dusty viscous fluid flow in a vertical channel saturated with porous medium subject to the convective boundary condition. The coupled partial differential equations are solved analytically using perturbation technique. The velocity, temperature and concentration fields have been studied for various combinations of physical parameters such as magnetic field, thermal radiation, Biot number and chemical reaction parameters. The expressions for skin friction, Nusselt number and Sherwood number are presented and the results are tabulated. Further, it is observed that the velocity profiles of dusty fluid are higher than the dust particles.

1. Introduction

Makinde and Chinyok[1] have analyzed the transport properties of a dusty fluid in a channel by accounting the electrical conductivity variations. Sivaraj and Rushi Kumar[2] have carried out a theoretical study to predict the influence of electric conductivity variations on Walters-B viscoelastic fluid flow.S ivaraj and Jasmine Benazir[3] have mathematically modeled the electrically conducting flow of a Casson fluid and analyzed the transport properties. JasmineBenazir and Sivaraj [4] have obtained a numerical solution for chemically reacting Casson fluid over a cone by employing the Crank–Nicolson technique.Mythili and Sivaraj [5] have used the implicit finite difference method to solve the governing equations which represent the chemically reacting Casson fluid flow. Animasaun et al [6] have analyzed the properties of the two chemically reacting species on viscoelastic fluid flow.The significance of thermal radiation on the Couette flow of a chemically reacting dusty Walters-B viscoelastic fluid in an asymmetric channel has been investigated by Sivaraj and RushiKumar[7].An analytical solution has been obtained by Prakash et al [8] to examine the characteristics of thermal radiation on a heat absorbing fluid flow. A theoretical investigation to explore the important role of nonlinear thermal radiation on thethermal boundary layer of a nanofluid has been carried out by Animasaun and Sandeep [9]. An attempt has been made by Kameswaran et al [10] to examine the influence of thenon-Darcy flow of a nanofluid over a vertical wavy surface. Stagnation point flow of nanofluid over porous medium has been analyzed by Kameswaran et al [11].Mythili et al [12] have mathematically modeled the non-Darcy flow of Casson fluid over two different geometries saturated with aporous medium.Makinde and Aziz [13] have investigated the nanofluid boundary layer flow over a sheet subject to convective heating boundary condition. Akbar et al [14] have numerically studied the flow of nanofluid over a cylinder by accounting the convective boundary condition.The

significance of convective boundary condition on the Couette flow of a chemically reacting dusty Walters-B viscoelastic fluid in an asymmetric channel has been investigated by Sivaraj and RushiKumar[15].Motivated by the above-mentioned investigations, in this paper, we investigate the transport properties of chemically reacting and thermally radiating magnetohydrodynamic flow of a dusty viscous fluid in a porous channel subject to convective boundary condition.

2. Formulation of the problem

The transport properties of time-dependent flow of an incompressible viscous fluid subject to natural convection in a vertical porous channel are modeled as depicted in Fig. 1.

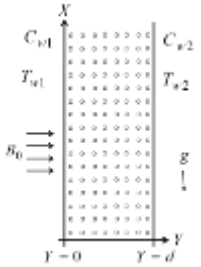

Figure 1. Flow Geometry

The fluid flow and uprightdirections are respectively represented by X-axis and Y-axis. The influence of an exterioreven magnetic field of strength B_0 applied at right angles, thermal radiation and first order chemically reactive species subject to thermal convective boundary conditions are analyzed. The governing equations which define the above-mentioned assumptions can be written as follows:

$$\frac{\partial U}{\partial t^*} = g\left(\beta_T (T - T_1) + \beta_C (C - C_1)\right) + \nu \frac{\partial^2 U}{\partial Y^2} + \frac{K_1 N_0}{\rho}(V - U) - \frac{\nu}{K^*} U - \frac{\sigma_e B_0^2}{\rho} U \tag{1}$$

$$\frac{\partial V}{\partial t^*} = -\frac{K_1}{m}(U - V) \tag{2}$$

$$\frac{\partial T}{\partial t^*} = \frac{1}{\rho C_P}\left(k \frac{\partial^2 T}{\partial Y^2} - \frac{\partial q_r}{\partial Y}\right) \tag{3}$$

$$\frac{\partial C}{\partial t^*} = D \frac{\partial^2 C}{\partial Y^2} - K_R (C - C_1) \tag{4}$$

The transport properties during primaryassumption $\left(t^* = 0\right)$ are

$$U = 0,\ V = 0,\ T = T_{w1},\ C = C_{w1} \text{ for } Y \in (0, d) \tag{5}$$

The transport properties atthe limits of the geometryat any time $\left(t^* > 0\right)$ are

$$U = 0, V = 0, -k\frac{\partial \mathrm{T}}{\partial Y} = h_f (T_{w1} + (T_{w2} - T_{w1})\varepsilon e^{-n^* t^*} - T), C = C_{w1} + (C_{w2} - C_{w1})\varepsilon e^{-n^* t^*} \text{ at } Y = 0 \tag{6}$$

$$U = 0, V = 0, -k\frac{\partial \mathrm{T}}{\partial Y} = h_f (T_{w2} + (T_{w2} - T_{w1})\varepsilon e^{-n^* t^*} - T), C = C_{w2} + (C_{w2} - C_{w1})\varepsilon e^{-n^* t^*} \text{ at } Y = d \tag{7}$$

The changein radiative heat is considered as $\frac{\partial q_r}{\partial Y} = 4(T - T_1)I',\ I' = \int_0^\infty K_{\lambda_1 w} \frac{\partial e_{b\lambda_1}}{\partial T} d\lambda_1$ (8)

where d is dimensional width of the channel, N_0 is number of density of the dust particles, K_1 is Stokes resistance coefficient, m is mass per unit volume of the dust particles, K^* is dimensional

porous permeability parameter, $K_{\lambda 1w}$ is coefficient ofradiation absorptionnear to walls, $e_{b\lambda 1}$ is Plank's function, K_R is the chemically reactive factor, n^* is real and positive constant and h_f is heat transfer coefficient.

The following quantitiesare introduced to obtain the dynamical similarity

$$x=\frac{X}{d},\ y=\frac{Y}{d},\ u=\frac{U}{U_0},\ v=\frac{V}{U_0},\ \theta=\frac{T-T_1}{T_2-T_1},\ \phi=\frac{C-C_1}{C_2-C_1},\ t=\frac{\nu t^*}{d^2},\ n=\frac{n^* d^2}{\nu} \tag{9}$$

Based on Eq. (9), the basic governing Eqs. (1)–(4) are summarized as following

$$\frac{\partial u}{\partial t}=\frac{\partial^2 u}{\partial y^2}+\frac{\delta}{w}(v-u)-Nu+G_r\theta+G_c\phi \tag{10}$$

$$w\frac{\partial v}{\partial t}=v-u \tag{11}$$

$$P_r\frac{\partial \theta}{\partial t}=\frac{\partial^2 \theta}{\partial y^2}+F\theta \tag{12}$$

$$S_c\frac{\partial \phi}{\partial t}=\frac{\partial^2 \phi}{\partial y^2}-K_r S_c\phi \tag{13}$$

The corresponding initial and boundary conditions (5)-(7) in dimensionless form are

$$t=0:\ u=0=v,\theta=0,\ \phi=0 \text{ for } t=0 \tag{14}$$

$$t>0:\ u=0=v,\ \theta'=B_i(\theta-\varepsilon e^{-nt}),\ \phi=\varepsilon e^{-nt} \text{ at } y=0 \tag{15}$$

$$u=0=v,\ \theta'=B_i(\theta-1-\varepsilon e^{-nt}),\ \phi=1+\varepsilon e^{-nt} \text{at } y=1 \tag{16}$$

The mass concentration of dust particle(δ), relaxation time parameter for particles(w), aparameter for themagnetic field (M^2), thermal Grashof number(G_r),porouspermeability coefficient (K), solutal Grashof number(G_c), Prandtl number(P_r), Biot number(B_i), Schmidt number and chemically reactivefactor(K_r) are respectively as follows:

$$\delta=\frac{mN_0}{\rho},\ w=\frac{m\nu}{K_1 d^2},\ M^2=\frac{\sigma_e B_0^2 d^2}{\mu},\ G_r=\frac{g\beta_T(T_2-T_1)d^2}{\nu U_0},\ \frac{1}{K}=\frac{d^2}{K^*},\ G_c=\frac{g\beta_C(C_2-C_1)d^2}{\nu U_0},$$

$$P_r=\frac{\mu C_P}{k},\ B_i=\frac{h_f d}{k},\ F=\frac{-4I'd^2}{k},\ S_c=\frac{\nu}{D},\ K_r=\frac{K_R d^2}{\nu}.$$

3. Method of solution

The analytical solutions are obtained for Eqs. (10)–(13) by adopting perturbation method. The fluid velocity(u), fluid temperature(θ) and fluid concentration(ϕ) can be represented in power of ε (ε << 1) as follows:

$$u(y,t)=u_0(y)+\varepsilon e^{-nt}u_1(y,t)+o(\varepsilon^2);\qquad v(y,t)=v_0(y)+\varepsilon e^{-nt}v_1(y,t)+o(\varepsilon^2);$$

$$\theta(y,t)=\theta_0(y)+\varepsilon e^{-nt}\theta_1(y,t)+o(\varepsilon^2);\qquad \phi(y,t)=\phi_0(y)+\varepsilon e^{-nt}\phi_1(y,t)+o(\varepsilon^2) \tag{17}$$

By means ofEq. (17) followed by neglectinghigher powers of o(ε^2), the Eqs. (10)–(16) becomes

$$u_0''-Nu_0=-(G_r\theta_0+G_c\phi_0);\qquad u_1''-(N-n)u_1=-(G_r\theta_1+G_c\phi_1) \tag{18}$$

$$\theta_0'' - F\theta_0 = 0; \qquad \theta_1'' - (F - nP_r)\theta_1 = 0 \tag{19}$$

$$\phi_0'' - K_r S_c \phi_0 = 0; \qquad \phi_1'' - (K_r - n)S_c \phi_1 = 0 \tag{20}$$

The appropriate boundary conditions become

$$u_0 = 0 = v_0,\ \theta_0' = B_i\theta_0,\ \phi_0 = 0,\ u_1 = 0 = v_1,\ \theta_1' = B_i(\theta_1 - 1),\ \phi_1 = 1 \text{ at } y = 0 \tag{21}$$

$$u_0 = 0 = v_0,\ \theta_0' = B_i(\theta_0 - 1),\ \phi_0 = 1,\ u_1 = 0 = v_1,\ \theta_1' = B_i(\theta_1 - 1),\ \phi_1 = 1 \text{ at } y = 1 \tag{22}$$

The Eqs. (18)–(20) are solved subject to the boundary conditions stated in Eqs. (21) and (22), and the expressions for the transport properties of the fluid are summarized as follows

$$\begin{aligned} u(y,t) = {} & (A_5 e^{\beta_1 y} + A_6 e^{\beta_2 y} + A_7 e^{\beta_3 y} + A_8 e^{\beta_4 y} + A_9 e^{\beta_5 y} + A_{10} e^{\beta_6 y}) \\ & + \varepsilon e^{-nt}(A_{15} e^{\beta_7 y} + A_{16} e^{\beta_8 y} + A_{17} e^{\beta_9 y} + A_{18} e^{\beta_{10} y} + A_{19} e^{\beta_{11} y} + A_{20} e^{\beta_{12} y}) \end{aligned} \tag{23}$$

$$\begin{aligned} v(y,t) = {} & (A_5 e^{\beta_1 y} + A_6 e^{\beta_2 y} + A_7 e^{\beta_3 y} + A_8 e^{\beta_4 y} + A_9 e^{\beta_5 y} + A_{10} e^{\beta_6 y}) \\ & + \frac{\varepsilon e^{-nt}}{1 - nw}(A_{15} e^{\beta_7 y} + A_{16} e^{\beta_8 y} + A_{17} e^{\beta_9 y} + A_{18} e^{\beta_{10} y} + A_{19} e^{\beta_{11} y} + A_{20} e^{\beta_{12} y}) \end{aligned} \tag{24}$$

$$\theta(y,t) = (A_3 e^{\beta_3 y} + A_4 e^{\beta_4 y}) + \varepsilon e^{-nt}(A_{13} e^{\beta_9 y} + A_{14} e^{\beta_{10} y}) \tag{25}$$

$$\phi(y,t) = (A_1 e^{\beta_1 y} + A_2 e^{\beta_2 y}) + \varepsilon e^{-nt}(A_{11} e^{\beta_7 y} + A_{12} e^{\beta_8 y}) \tag{26}$$

where $N = K^{-1} + M^2$; $\beta_1 = -\beta_2 = \sqrt{K_r S_c}$; $\beta_3 = -\beta_4 = \sqrt{F}$; $\beta_5 = -\beta_6 = \sqrt{N}$;

$\beta_7 = -\beta_8 = \sqrt{(K_r - n)S_c}$; $\beta_9 = -\beta_{10} = \sqrt{F - nP_r}$; $\beta_{11} = -\beta_{12} = \sqrt{N - n}$; $A_1 = \left(e^{\beta_1} - e^{\beta_2}\right)^{-1}$;

$A_2 = e^{\beta_2}\left(e^{\beta_2} - e^{\beta_1}\right)^{-1}$; $A_3 = -B_i\left(\beta_3 - B_i\right)^{-1}\left(e^{\beta_3} - e^{\beta_4}\right)^{-1}$; $A_4 = -B_i\left(\beta_4 - B_i\right)^{-1}\left(e^{\beta_4} - e^{\beta_3}\right)^{-1}$;

$A_5 = -A_1 G_c\left(\beta_1^2 - N\right)^{-1}$; $A_6 = -A_2 G_c\left(\beta_2^2 - N\right)^{-1}$; $A_7 = -A_3 G_r\left(\beta_3^2 - N\right)^{-1}$; $A_8 = -A_4 G_r \beta_4^2 - N$;

$A_9^* = A_5\left(e^{\beta_1} - e^{\beta_6}\right) + A_6\left(e^{\beta_2} - e^{\beta_6}\right) + A_7\left(e^{\beta_3} - e^{\beta_6}\right) + A_8\left(e^{\beta_4} - e^{\beta_6}\right)$; $A_9 = -A_9^*\left(e^{\beta_5} - e^{\beta_6}\right)^{-1}$;

$A_{10}^* = A_5\left(e^{\beta_1} - e^{\beta_5}\right) + A_6\left(e^{\beta_2} - e^{\beta_5}\right) + A_7\left(e^{\beta_3} - e^{\beta_5}\right) + A_8\left(e^{\beta_4} - e^{\beta_5}\right)$; $A_{10} = -A_{10}^*\left(e^{\beta_6} - e^{\beta_5}\right)^{-1}$;

$A_{11} = \dfrac{-e^{\beta_8}}{e^{\beta_7} - e^{\beta_8}}$; $A_{12} = \dfrac{-e^{\beta_7}}{e^{\beta_8} - e^{\beta_7}}$; $A_{13} = \dfrac{B_i\left(e^{\beta_{10}} - 1\right)}{\left(\beta_9 - B_i\right)\left(e^{\beta_9} - e^{\beta_{10}}\right)}$; $A_{14} = \dfrac{B_i\left(e^{\beta_9} - 1\right)}{\left(\beta_{10} - B_i\right)\left(e^{\beta_{10}} - e^{\beta_9}\right)}$;

$A_{15} = \dfrac{-A_{13} G_c}{\beta_7^2 - N - n}$; $A_{16} = \dfrac{-A_{14} G_c}{\beta_8^2 - N - n}$; $A_{17} = \dfrac{-A_{13} G_r}{\beta_9^2 - N - n}$; $A_{18} = \dfrac{-A_{14} G_r}{\beta_{10}^2 - N - n}$;

$A_{19}^* = A_{15}\left(e^{\beta_7} - e^{\beta_{12}}\right) + A_{16}\left(e^{\beta_8} - e^{\beta_{12}}\right) + A_{17}\left(e^{\beta_9} - e^{\beta_{12}}\right) + A_{18}\left(e^{\beta_{10}} - e^{\beta_{12}}\right)$; $A_{19} = -A_{19}^*\left(e^{\beta_{11}} - e^{\beta_{12}}\right)^{-1}$;

$A_{20}^* = A_{15}\left(e^{\beta_7} - e^{\beta_{11}}\right) + A_{16}\left(e^{\beta_8} - e^{\beta_{11}}\right) + A_{17}\left(e^{\beta_9} - e^{\beta_{11}}\right) + A_{18}\left(e^{\beta_{10}} - e^{\beta_{11}}\right)$; $A_{20} = -A_{20}^*\left(e^{\beta_{12}} - e^{\beta_{11}}\right)^{-1}$

The rate of fluid velocity (τ), the rate of heat transfer (Nu) and the rate of mass transfer(Sh) at wall $y = 0$ and wall $y = 1$ are given by

$$\tau_{f0} = -u'|_{y=0},\ \tau_{f1} = -u'|_{y=1}; \qquad \tau_{p0} = -v'|_{y=0},\ \tau_{p1} = -v'|_{y=1};$$

$$Nu_0 = -\theta'|_{y=0},\ Nu_1 = -\theta'|_{y=1}; \qquad Sh_0 = -\phi'|_{y=0},\ Sh_1 = -\phi'|_{y=1} \tag{27}$$

4. Result and discussions

Figures2 and 3depict the flow, heat and mass transfer characteristics of the problem. Throughout the computations we employ w = 10, G_r = 2, M = 2, G_c = 1, K = 2, P_r = 0.71, S_c = 0.96, Bi = 0.1, ε = 0.02,t = 1, F = 2, and K_r = 2 unless otherwise stated.

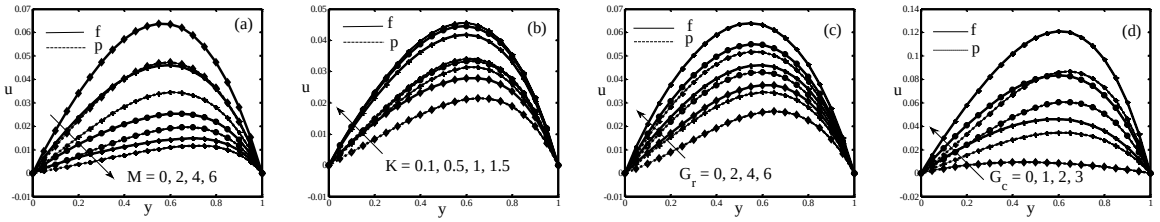

Figure 2. Velocity Profiles

Figure 2(a)-2(d) present the influence of M, K, G_r and G_c on fluid velocity distributions of dusty fluid and dust particles. Fig. 2(a) shows that the magnifying the strength of magnetic field parameter lead to diminishing the flow of the dusty fluid as well as dust particles. Near to both end of the channels, the effect is less compared with the center of the channel. It is clear from Fig. 2(b) that increases in porosity parameter speed up the fluid flow by condensingstraindynamism. Figs. 2(c) and 2(d) illustrate that the higher values of thermal Grashof number and solutal Grashof numberaccelerate the flow of the dusty fluid and dust particles.

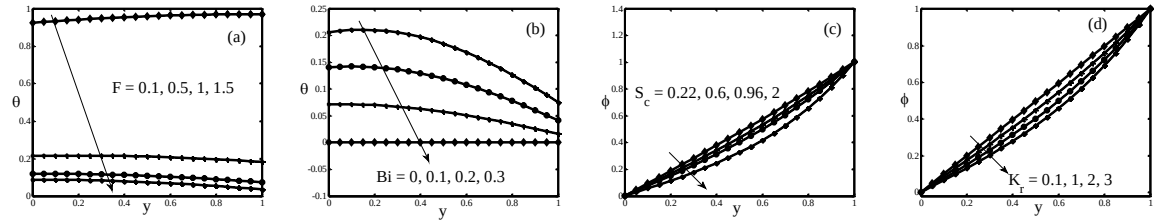

Figure 3. Temperature and Concentration Profiles

Figures 3(a) and 3(b) present the effects of F and Bi on the temperature distribution, respectively. Fig. 3(a) represents that magnifying the thermal radiation parameter ardently diminish the heat transfer within the channel by emitting more heat outside the channel. Fig. 3(b) elucidates that increase in Biot number decrease the heat transfer. the effects of S_c and K_r on the concentration distribution are presented in Figures 3(c) and 3(d), respectively. Fig. 3(c) elucidates that higher values of Schmidt decrease the fluid concentration. It is observed from the Fig. 3(d) that strengthening the chemical reaction parameter drops the fluid concentration. Table 1 illustrates the variations of skin friction at the walls $y = 0$ and $y = 1$for different values of M and w. Table 2 displays the variations of skin friction and rate of heat transfer distributions near walls $y = 0$ and $y = 1$ for the pertinent parameters F and Bi. Table 3 shows the variations of skin friction and rate of mass transfer distributions near walls $y = 0$ and $y = 1$ for different values of S_c and K_r.

Table 1. Variations of *M* and *w*on τ_{f0}, τ_{p0}, τ_{f1} and τ_{p1}. (PP – Physical Parameter)

PP	Values	τ_{f0}	τ_{p0}	τ_{f1}	τ_{p1}
M	0	-0.1944	-0.1796	0.3349	0.3215
	2	-0.1392	-0.1276	0.2714	0.2611
	4	-0.0764	-0.0687	0.1904	0.1839
w	1	-0.1392	-0.1407	0.2714	0.2727
	2	-0.1392	-0.1431	0.2714	0.2749
	3	-0.1392	-0.1479	0.2714	0.2792

Table 2. Effect of *F* and *Bi*on τ_{f0}, τ_{p0}, τ_{f1}, τ_{p1}, Nu_0 and Nu_1.

PP	Values	τ_{f0}	τ_{p0}	τ_{f1}	τ_{p1}	Nu_0	Nu_1
F	0	-7.7180	-7.7050	8.1788	8.1669	-0.9986	-0.9985
	2	-0.0595	-0.0484	0.1951	0.1849	0.0052	0.1102
	4	-0.0778	-0.0666	0.2161	0.2057	0.0030	0.1072
Bi	0	-0.0913	-0.0805	0.2419	0.2311	0.0000	0.0000
	0.1	-0.1392	-0.1276	0.2714	0.2611	-0.0056	0.1001
	0.2	-0.1866	-0.1760	0.3061	0.2960	-0.0253	0.1953

Table 3. Effect of S_c and K_r on τ_{f0}, τ_{p0}, τ_{f1}, τ_{p1}, Sh_0 and Sh_1.

PP	Values	τ_{f0}	τ_{p0}	τ_{f1}	τ_{p1}	Sh_0	Sh_1
S_c	0.22	-0.1559	-0.1432	0.2918	0.2804	-0.9271	-1.1457
	0.6	-0.1471	-0.1350	0.2812	0.2704	-0.8167	-1.3794
	0.96	-0.1400	-0.1283	0.2724	0.2620	-0.7271	-1.5831
K_r	0	-0.1617	-0.1484	0.2987	0.2867	-0.0016	-0.9984
	1	-0.1494	-0.1370	0.2839	0.2729	-0.8448	-1.3192
	2	-0.1392	-0.1276	0.2714	0.2611	-0.7180	-1.6048

5. Conclusions

Analytical solutions are obtained for the magnetohydrodynamic flow of thermally radiating and chemically reacting dusty viscous fluid in an irregular channel subject to the convective boundary condition. The important observations of this investigation are as follows: The dusty fluid velocity is higher than the dust particles velocity. The flow and heat transfer profiles strictly decrease for increasing F and Bi. An increase in Kr diminishes the flow and mass transfer profiles. Velocity profiles enhance for increasing K, Gr and Gc but they decrease for increasing M.

References

[1] Makinde OD and Chinyok T 2010Comput Math Appl 60 660.
[2] Sivaraj R and RushiKumar B 2013 Int J Heat Mass Transfer 61 119.
[3] Sivaraj R and JasmineBenazir A 2015 Special Topics Reviews Porous Media 6 267–281
[4] JasmineBenazir A and Sivaraj R 2016 Adv Intelligent Systems Comput 436 537.
[5] Mythili D and Sivaraj R 2016 J MolLiq 216 466.
[6] Animasaun IL, Raju CSK and Sandeep N 2016 Alexandria Engng J 55 1595.
[7] Sivaraj R and Rushi Kumar B 2012 Int J Heat Mass Transfer 55 3076.
[8] Prakash J, RushiKumar B, Sivaraj R 2014 Walailak J Science Tech 11 939.
[9] Animasaun IL and Sandeep N 2016 Powder Tech 301 858.
[10] Kameswaran PK, Vasu B, Murthy PVSN and Gorla RSR 2016 IntCommun Heat Mass Transfer 77 78
[11] Kameswaran PK, Sutradhar A, Murthy PVSN and Sibanda P 2016 J Nanofluids 5 310.
[12] Mythili D, Sivaraj R and Rashidi MM 2017 Int J Numerical Methods Heat Fluid Flow 27 156.
[13] MakindeOD and AzizAInt J Thermal Sci 50 1326.
[14] Akbar NS, Nadeem S, Haq RU and Khan ZH 2013 Chinese J Aeronautics 26 1389
[15] Sivaraj R and Rushi Kumar B 2012 Int J Heat Mass Transfer 55 3076.